İnönü Üniversitesi Sağlık Hizmetleri Meslek Yüksekokulu Dergisi
ISSN: 2147-7892, Cilt 9, Sayı 3 (2021) 862-872
doi: 10.33715/inonusaglik.941224

Journal of Inonu University Health Services Vocational School
ISSN: 2147-7892, Volume 9, Issue 3 (2021) 862-872
doi: 10.33715/inonusaglik.941224

Original Article / Araştırma Makalesi

ST. JOHN'S WORT (*HYPERICUM PERFORATUM* L.) FLOWER BASED CARBON/GRAPHENE QUANTUM DOT STRUCTURE PRODUCTION AND CHARACTERIZATION FOR BIOIMAGING AND DRUG DELIVERY SYSTEMS

Biyogörüntüleme ve İlaç Taşıyıcı Sistemler için Sarı Kantaron (*Hypericum perforatum* L.) Çiçeği Temelli Karbon/Grafen Kuantum Dot Yapı Eldesi ve Karakterizasyonu

İdil KARACA AÇARI[1] *Yunus ÖNAL*[2]
[1]*Malatya Turgut Özal University, Faculty of Engineering and Natural Sciences, Malatya*
[2]*İnönü University, Faculty of Engineering, Malatya*

Geliş Tarihi / Received: *23.05.2021* ***Kabul Tarihi / Accepted:*** *02.11.2021*

ABSTRACT

In this study, it was aimed to obtain carbon and graphene quantum dot structures from St. John's Wort (*Hypericum perforatum* L.) flowers, originating from the city of Hatay. *Hypericum perforatum* L. flower sample was subjected to carbonization at different temperatures such as 200, 225 and 250 ℃ for the desired quantum dot structure yields. It has been observed that the best radiation after carbonization is at 250 ℃. Fourier transform infrared spectrometer, X-ray diffraction and scanning electron microscopy techniques were used to determine the structural characterizations and surface morphology, respectively. The UV radiation of *Hypericum perforatum* L. flower-based carbon and graphene quantum structures was followed at 365 nm and the blue glow was observed very clearly. With this study, quantum and graphene dot structures based on *Hypericum perforatum* L. flower have been introduced to the literature for the first time. In addition, the quantum dot structures with blue radiation obtained within the scope of the study will be an alternative reference for many bioimaging and drug delivery system studies.

Keywords: Carbonization, Quantum dots, St. John's Wort (*Hypericum perforatum* L.) flower.

ÖZ

Bu çalışmada, Hatay ilinden toplanan sarı kantaron (*Hypericum perforatum* L.) çiçeklerinden karbon ve grafen kuantum dot yapıların elde edilmesi amaçlanmıştır. *Hypericum perforatum* L. çiçek örneği, istenilen kuantum dot yapı eldeleri için 200, 225, 250 ℃ gibi farklı sıcaklıklarda karbonizasyon işlemine tabi tutulmuştur. Karbonizasyon sonrası en iyi ışımanın 250 ℃'de olduğu gözlemlenmiştir. Yapısal karakterizasyonlarda ve yüzey morfoloji belirlenmesinde sırasıyla fourier dönüşümü kızılötesi spektrometre, X-ışını kırınımı ve taramalı elektron mikroskobu teknikleri kullanılmıştır. *Hypericum perforatum* L. çiçek temelli karbon ve grafen kuantum yapılarına ait UV ışıma ise 365 nm de takip edilmiş ve mavi renkli olan ışıma oldukça net bir şekilde gözlemlenmiştir. Yapılan çalışma ile ilk kez *Hypericum perforatum* L. çiçeği temelli kuantum ve grafen dot yapılar literatüre kazandırılmıştır. Buna ek olarak, çalışma kapsamında elde edilen mavi ışıma yapan kuantum dot yapılar pek çok biyogörüntüleme ve ilaç taşıyıcı sistem çalışmalarına alternatif bir referans olacaktır.

Anahtar kelimeler: Karbonizasyon, Kuantum noktalar, Sarı kantaron (*Hypericum perforatum* L.) çiçeği.

İdil KARACA AÇARI ✉, *idil.karaca@ozal.edu.tr*
Malatya Turgut Özal University, Faculty of Engineering and Natural Sciences, Malatya

Bu makaleye atıf yapmak için(How to cite this article): Karaca Açarı, İ., Önal, Y. (2021). St. John's Wort (*Hypericum perforatum* L.) Flower Based Carbon/Graphene Quantum Dot Structure Production and Characterization for Bioimaging and Drug Delivery Systems. İnönü Üniversitesi Sağlık Hizmetleri Meslek Yüksekokulu Dergisi, 9(3), 862-872. doi: 10.33715/inonusaglik.941224

INTRODUCTION

Quantum Dots (QDs) are nano-sized semiconductor crystals **(**Kargozar & Mozafari, 2018; Zheng, Ananthanarayanan, Luo, & Chen, 2015). QDs were first discovered by a Russian physicist Alexei Ekimov in the 1980s (Pohanka, 2017). QDs have unique optical properties due to the quantum and dimensional effect. This property makes them suitable for use as luminescent nanoprops and carriers in biological applications (Abbaspourrad, Datta, & Weitz, 2013; Peer et al., 2007). In addition, QDs are widely used in the fields of biology and medicine in recent years. QDs are used in many fields such as drug delivery-targeting, detection of DNA and oligonucleotides, molecular histopathology, flow cytometry-based detection, disease diagnosis and biological imaging (Wagner, Knipe, Orive, & Peppas, 2019). Carbon and / or graphene quantum dots (CQD, GQD), one of the members of the Quantum Dot family, has gained worldwide attention since its discovery in 2004 (Xu et al., 2004). CQDs are described as a fascinating class of carbon nanoparticles composed of nanosized carbons (Xue et al., 2019). CQDs have the potential to apply in many fields (biomedical, photocatalyst, etc.) due to their high stability, good biocompatibility, high dispersibility in water, low cost and excellent photostability (Cayuela et al., 2015; Das, Bandyopadhyay, & Pramanik, 2018; Du, Zeng, Ming, & Wu, 2013; Lim, Liu, Kim, & Son, 2018; Lin et al., 2012; Liu et al., 2015; Shahla, Masoud, & Davood, 2018; Tian et al., 2009; Wang, Liu, Zhang, & Lv 2012; Wang & Zhou, 2014; Yang et al., 2009; Yong, 2009). The adjustable fluorescence and quantum size effect of CQDs make them promising materials for observing various cellular processes and biological imaging (Kargozar et al., 2020). When we look at the biomedical application areas of CQDs, drug delivery, cellular imaging, bioimaging, biosensor, bacterial imaging and targeting, gene distribution, radiotherapy, phototherapy can be given as examples (Devi, Saini, & Kim, 2019).

In the graphene quantum dot structures, another member of the quantum dot family, attracts grena attention especially in biomedical field uses due to its unique physicochemical properties and extraordinary biocompatibility (Chen et al., 2017). The unique electronic structure of GQDs gives these nanomaterials functional properties such as powerful, adjustable photoluminescence for fluorescent bio-imaging and biosensing use, and their use in drug delivery systems (Chung, Revia, & Zhang, 2019). In this study, *Hypericum perforatum* L. flower was used as a raw material source in the preparation of both CQD and GQD structures. *Hypericum perforatum* L. is a member of the genus *Hypericum*, which has 400 species worldwide. It is native to Europe, Western Asia, North Africa, Madeira, and the Azores Islands. It is found naturally in many region of the world, especially in North America and Australia.

The consumption of *Hypericum perforatum* L. derivative products has increased significantly in recent years and are now one of the most consumed medicinal plants (Ekren, Sonmez, & Bayram, 2010).

The aim of this study is to present alternative, low-cost CQD and GQD structures for bioimaging and drug delivery systems. For this purpose, thermal carbonization method, which is widely used, was used to obtain both CQD and GQDs from *Hypericum perforatum* L. flowers, which originate in the province of Hatay. The characterization and surface morphology properties of the obtained quantum dot structures were determined by known appropriate techniques.

MATERIAL AND METHOD

The study is based on two experimental groups. The first is the group consisting of crude *Hypericum perforatum* L. flowers, the second group is the obtained CQD and GQD structures at different temperatures (200, 225 and 250 ℃). The characterization step of the samples was carried out for *Hypericum perforatum* L. flower based quantum dot structures that give the best UV radiation (irradiance at 250 ℃) at the temperatures determined by the crude *Hypericum perforatum* L. flower sample. In the characterization steps, the fourier transform infrared spectrometer (FTIR) spectrum was recorded on a Perkin Elmer Spectrum Two model Fourier Transform Infrared Spectrometer in the range 4000-400 cm^{-1}. The qualitative and quantitative analyzes of the samples were carried out by the X-Ray Diffraction method (XRD, Rigaku Miniflex II model). Surface morphologies were obtained with high resolution images using Leo EV40 brand scanning electron microscope (SEM) device. Finally, the radiation obtained from an excitation 365 nm with the UV lamp (Perkin Elmer Lambda 25) was determined with the sample containing the CQD and GQD structures based on *Hypericum perforatum* L. flower.

Preparation of CQD and GQD

Dried flower parts of *Hypericum perforatum* L. belonging to Hatay region were collected. Samples consisting of dried and dust-free *Hypericum perforatum* L. flowers were subjected to carbonization process. The carbonization process was carried out at different temperatures (200, 225 and 250 ℃) for 3h. For the carbonization process, approximately 1g of dried *Hypericum perforatum* L. flowers were spread homogeneously in a glass petri dish and carbonized in the air using an ash oven at the temperatures given above (Önal, Kır, Dehri, & Esen, 2019).

Measurement with UV Lamp

Carbonized *Hypericum perforatum* L. flower samples were prepared as 0.3g/50mL solution in deionized water. After an average of 12h of stirring at 400 rpm, the prepared samples were filtered through a 0.45 micron filter and the stimulation luminescence at 365 nm were observed in a UV lamp.

RESULTS

FTIR Results

When the FTIR spectra of the raw and carbonized *Hypericum perforatum* L. flowers are examined in Figure 1, it is seen that there are significant changes in the functional structure and hence macromolecular structure as a result of heat treatment. The wide peak seen at ~ near 1018 cm^{-1} belongs to C-O or C-O-C structures. The decrease of this peak at the disappearance point after the carbonization process indicates that this peak belongs to the organic groups in the structure. In other words, there are no inorganic components in the structure. Because, inorganic M-O-M stretches are also seen specifically in the region of ~ near 1018 cm^{-1}. The sharp peak around 1731 cm^{-1} is caused by the carbonyl C = O stretching of aldehyde structures that do not belong to carboxyl groups. The aldehyde structure of the fragrance components in the flower structure confirms this peak. In addition, this peak belongs to C = O stretching in unconjugated ketones, carbonyls and ester groups in natural materials and C = O stretching of conjugated aldehydes and carboxylic acids. The two peaks observed at 2919 and 2852 cm^{-1} belong to the asymmetric and symmetrical aliphatic C-H stretching. It belongs to the OH stretching in all organic structures, including broadband water with a peak minimum of ~ near 3257 cm^{-1}. It belongs to the peak C-H deformation stretching around 1376 cm^{-1}. The coexistence of 1730 and 1380 cm^{-1} peaks indicates that the C = O structure of aldehyde is present in the flower structure. It belongs to C = C structures in wide band alkene structure around 1596 cm^{-1}. When the FTIR spectrum of the carbonized *Hypericum perforatum* L. flower is examined, it is seen that the units belonging to the functional groups in the structure are separated from the structure. In the 3257 cm^{-1} region, a rather flat and weak peak -OH stretching peak is observed (Murru, Badía-Laíño, & Díaz-García, 2020; Zarrinbakhsh, Mohanty, & Misra, 2013). The peak presence indicates the presence of organic structures that still have OH groups in the structure. Looking at the carbonized structure, the peak corresponding to the C-H bonds in the methyl or methylene groups is seen at near 2894 cm^{-1} (Murru et al., 2020). The peak is poorly seen. It can be interpreted as an indication that the aliphatic structures in this structure are not fully degraded.

The region of 1800 – 900 cm^{-1} indicates the still existence of basic organic units in the structure. Therefore, the fact that the water extract of the carbonized *Hypericum perforatum* L. flowers radiates at 365 nm can be explained by the presence of nano-organic structures remaining in the structure. As a matter of fact, it can be stated that the macromolecular structure maintains the similarity with the FTIR spectrum of the crude and carbonized solids being completely similar.

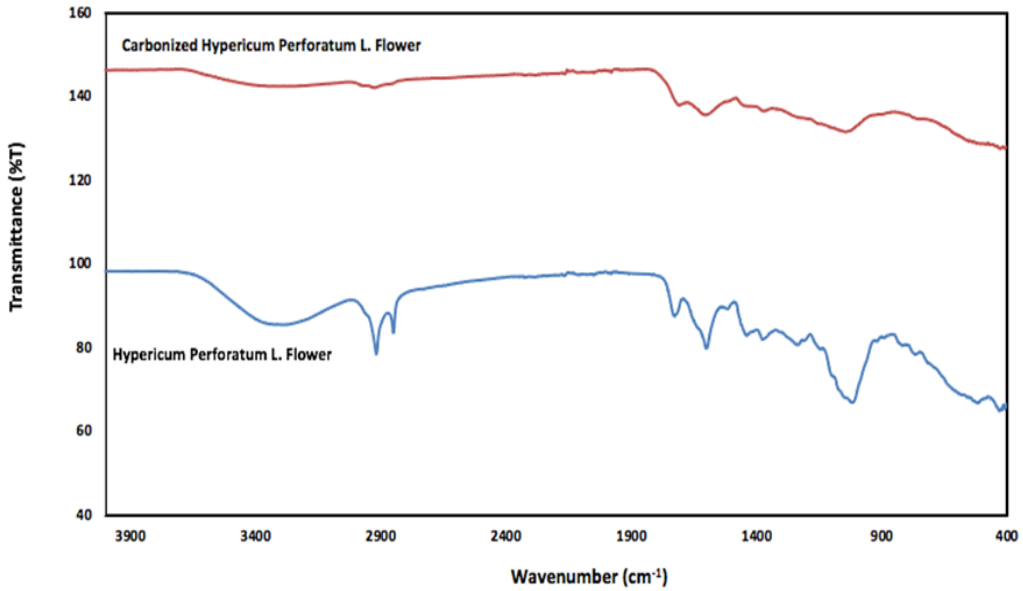

Figure 1. FTIR spectra of *Hypericum perforatum* L. flower and *Hypericum perforatum* L. flower carbonized at 250 ℃.

XRD Results

When the XRD graph of raw and carbonized Hypericum perforatum L. flower samples is examined in Figure 2, it is seen that the raw sample is both crystalline and amorphous.. The wide splay peak with a peak maximum of 2θ = 23º belongs to amorphous and crystalline cellulosic structures in natural samples (Ahvenainen, Kontro, & Svedstro¨m, 2016). In this structure, it is seen that they are mostly in crystalline units, although they are mostly amorphous structures. It can be stated that *Hypericum perforatum* L. flower has a single macromolecular structure as well as very different crystalline units. There is a separate macromolecular unit around 2θ=43º albeit very small. Although the carbonization temperature is not high, it is clearly seen that there is a structural arrangement when the mass loss is taken into account. The peak with a peak maximum of 2θ = 23º gets wider and crystalline units decrease. As a result, the second macromolecular unit around 2θ = 43º clearly emerges. Although the carbonized sample shows a similar structure to the raw sample, it is seen that a new macromolecular structure has been formed around 2θ = 43º due to the separated units due to mass reduction.

This peak belongs to graphite and graphene structures (Kigozi et al., 2020). All the characterizations made are in accordance with the literature.

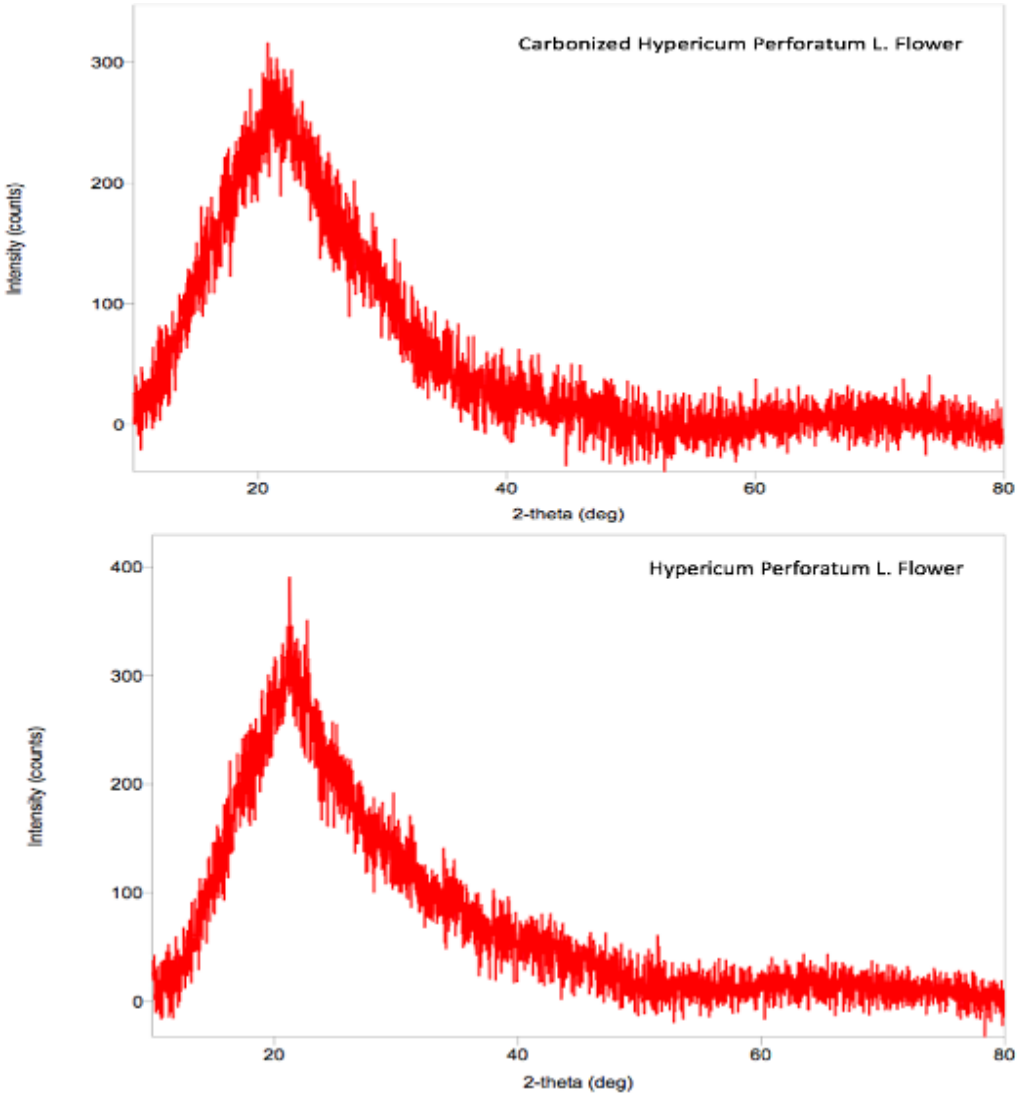

Figure 2. XRD results of carbonized at 250 ℃ *Hypericum perforatum* L. flower and raw *Hypericum perforatum* L. flower.

SEM Results

According to the SEM image of the crude *Hypericum perforatum* L. flower given in Figure 3a, the surface morphology is quite homogeneous and the structural sequences are clearly seen in the figure. It is clearly seen that when carbonized, these homogeneous structural units break down and there is a new structural arrangement due to the removal of materials with low boiling point. The graphene structure is clearly visible as a result of carbonization.

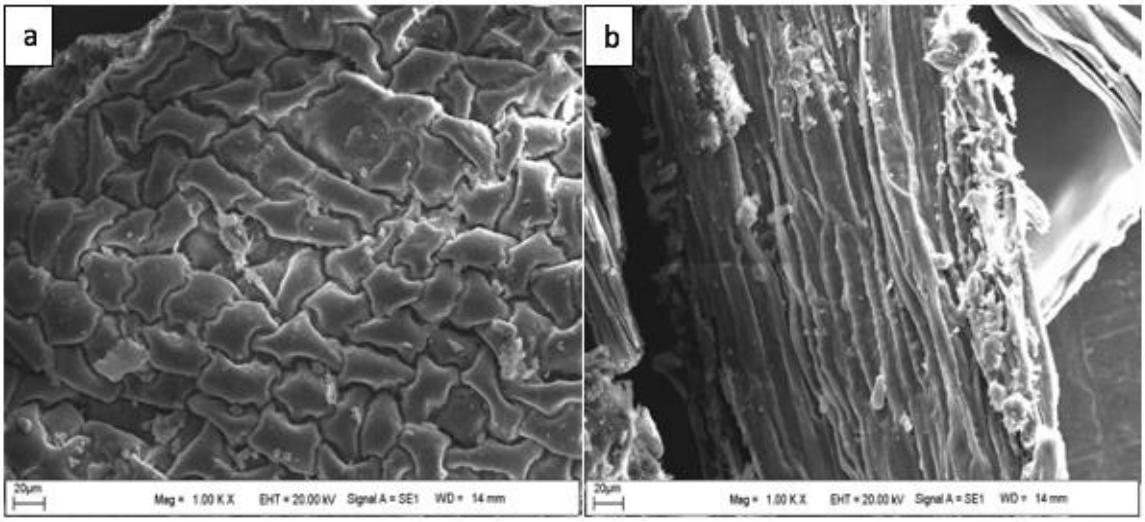

Figure 3. SEM images of *Hypericum perforatum* L. flower (a) and *Hypericum perforatum* L. flower carbonized at 250 ℃ (b).

UV Cabinet Images

Hypericum perforatum L. flower based samples prepared at different temperatures (200, 225 and 250 ℃) were irradiation in a UV cabinet at 365 nm wavelength. These irradiation taken are given in Figure 4.

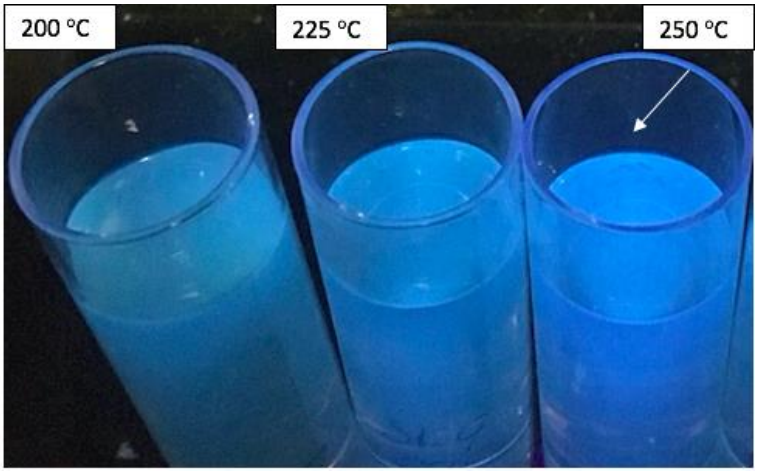

Figure 4. UV cabinet images of carbonized *Hypericum perforatum* L. flower samples.

When Figure 4 is examined, the fluorescence radiations in the aqueous solution are clearly seen for all three carbonization temperatures. Considering that the amount of carbonized solid prepared with pure water is the same, it can be stated that irradiation is higher at 250 ℃, and therefore more carbon spots are formed at this temperature. When we look at Figure 5, we see that the samples are irradiated in daylight and in the UV cabinet.

Figure 5. Daylight of *Hypericum perforatum* L. flower carbonized at 250 ℃ and UV irradiation image at 365 nm wavelength

DISCUSSION

In this study, carbon/graphene dots structures obtained from *Hypericum perforatum* L. flower have been studied for the first time in the literature. Therefore, discussion has been interpreted by comparing with carbon/graphene structures obtained from different plants. When we look at the crude *Hypericum perforatum* L. flower sample, Taraj et al. observed the incoming band ~ near 1731 cm^{-1} at ~ near 1730 cm^{-1} and expressed it as the C = O vibration originating from the ketone functional group (Taraj et al., 2019). Studies conducted on the C = O vibration originating from the ketone functional group are based on hypericin and hyperforin. This finding is in good agreement with studies on FTIR analysis of hypericin (Baciu, Ranga, Fetea, Zavoi, & Socacıu, 2013; Nikolic & Zlatkovic, 2010). In addition, Taraj et al. mention the presence of a peak due to CH_3 symmetrical bending around 1375 cm^{-1} (Taraj et al., 2019). The large peak seen at ~ 1018 cm^{-1} in *Hypericum perforatum* L. flower is due to the C-O or C-O-C structures of organic groups. The results are in line with the results given by Nandiyanto et al. (Nandiyanto, Oktiani, & Ragadhita, 2019). It confirms the presence of broadband hydroxyl groups at ~ near 3257 cm^{-1}. Jarzebski and colleagues observed strong-large hydroxyl groups in the range of 3500 to 3100 cm^{-1} in *Hypericum perforatum* L. (Jarzębski et al., 2020). The peak we observed at 2894 cm^{-1} belongs to the aliphatic C-H stretching corresponding to the methyl or methylene group. Jarzebski et al. observed the band corresponding to carbon-hydrogen bond stretching vibrations at ~ near 2930 cm^{-1}. Jarzebski et al. emphasized that the peak at ~ near 1600 cm^{-1} represents bonds in the carbonyl group (Jarzębski et al., 2020). When we look at the carbonized *Hypericum perforatum* L. flower, we see -OH peak at ~ near 3257

cm^{-1} and aliphatic C-H peak corresponding to methyl or methylene group at 2894 cm^{-1}. It is the absorption peaks of the C = O functional groups that are distinctive at 1574 cm^{-1} and very small at 1444 cm^{-1}, which are distinctive for CQDs. We see the C-N stretching peak around ~ 1327 cm^{-1} and the peak belonging to the C-O stretch vibration at 1029 cm^{-1}. All these comments are consistent with the FTIR comments of Pandiyan et al. (Pandiyan et al., 2020). *Hypericum perforatum* L. flower sample carbonized in XRD results shows similar structure to the crude *Hypericum perforatum* L. flower sample. In addition, it is easily seen in XRD results that a new macromolecular structure is formed around $2\theta = 43^{o}$ due to the units separated due to the mass reduction. In SEM images of *Hypericum perforatum* L. the homogeneity of the surface morphologies was distorted when carbonized, and a completely different surface morphology was observed. As a result of the interpretation of all these characterization processes, it has been proved that carbon/graphene structures based on *Hypericum perforatum* L. flower are obtained.

CONCLUSION

In recent years CQDs/GQDs have attracted increasing attention due to their properties such as fluorescence emission, small size, chemical stability, water solubility, easy synthesis and functionalization. Especially due to its small size, biocompatibility, adjustable photoluminescence properties, it can be monitored in the body and used as drug delivery devices (Molaei, 2019; Zheng et al., 2015). Different carbon dots were obtained from various natural sources (orange juice, lemon juice, papaya powder, orange peel, pollen, cane molasses, etc.) (Dinç & Kara, 2018). With this study, CQDs and GQDs structures were obtained for the first time from the flower of *Hypericum perforatum* L. which is used for many medical purposes. It is obvious that these structures with blue irradiation will have a high potential of use as a bio-imaging and drug delivery tool. Considering the widespread use of both yellow and red centaury plants in alternative medicine, it is of great importance to determine the carbon dots obtained with this study.

REFERENCES

Abbaspourrad, A., Datta, S. S., Weitz, D. A. (2013). Controlling release from pH- responsive microcapsules. Langmuir, 29, 12697–12702.

Ahvenainen, P., Kontro, I., Svedstro ̈m, K. (2016). Comparison of sample crystallinity determination methods by X-ray diffraction for challenging cellulose I materials. Cellulose, 23, 1073-1086.

Baciu, A., Ranga, F., Fetea, F., Zavoi, S., Socaciu, C. (2013). Fingerprinting food supplements and their botanical ingredients by coupled UV/Vis/FTIR Spectrometry. Bulletin UASVM Food Science and Technology, 70, 8.

Cayuela, A., Kennedy, S. R., Soriano, M. L., Jones, C. D., Valcarcel, M., Steed, J. W. (2015). Fluorescent carbon dot–molecular salt hydrogels. Chemical Science, 6, 6139–6146.

Chen, F., Gao, W., Qiu, X., Zhang, H., Liu, L., Liao, P., … Luo, Y. (2017). Graphene quantum dots in biomedical applications: Recent advances and future challenges. Frontiers in Laboratory Medicine, 1, 192-199.

Chung, S., Revia, R. A., Zhang, M. (2019). Graphene quantum dots and their applications in bioimaging, biosensing, and therapy. Advanced Materials, 33, 1904362.

Das, R., Bandyopadhyay, R., Pramanik, P. (2018). Carbon quantum dots from natural resource: A review. Materials Today Chemistry, 8, 96–109.

Devi, P., Saini, S., Kim, K-H. (2019). The advanced role of carbon quantum dots in nanomedical applications. Biosensors and Bioelectronics, 141, 111158.

Dinç, S., Kara, M. (2018). Synthesis and applications of carbon dots from food and natural products: A mini-review. Journal of Apitherapy and Nature, 1, 33-37.

Du, F. K, Zeng, F., Ming, Y. H., Wu, S. Z. (2013). Carbon dots-based fluorescent probes for sensitive and selective detection of iodide. Microchimica Acta, 180, 453–460.

Ekren, S., Sonmez, C., Bayram, E. (2010). Sarı Kantaron (Hypericum perforatum L. Klonlarında Bazı Tarımsal ve Kalite Özelliklerinin Belirlenmesi. Tarim Bilimleri Dergisi, C 16, 225-234

Jarzębski, M., Smułek, W., Baranowska, H. M., Masewicz, Ł., Kobus-Cisowska, J., Ligaj, M., Kaczorek, E. (2020). Characterization of St. John's wort (Hypericum perforatum L.) and the impact of filtration process on bioactive extracts incorporated into carbohydrate-based hydrogels. Food Hydrocolloids, 104, 105748.

Kargozar, S., Hoseini, S. J., Milan, P. B., Hooshmand, S., Kim, H-W., Mozafari, M. (2020). Quantum dots: A review from concept to clinic. Biotechnology Journal, 15(12), 2000117.

Kargozar S, Mozafari M. (2018). Nanotechnology and nanomedicine:start small, think big. Materials Today:Proceeding, 5, 15492-15500.

Kigozi, M., Koech, R. K., Kingsley, O., Ojeaga, I., Tebandeke, E., Kasozi, G. N., Onwualu, A. P. (2020). Synthesis and characterization of graphene oxide from locally mined graphite flakes and its supercapacitor applications. Results in Materials, 7, 100113.

Lim, H., Liu, Y., Kim, H. Y., Son, D. I. (2018). Facile synthesis and characterization of carbon quan- tum dots and photovoltaic applications. Thin Solid Films, 660, 672–677.

Lin, L. P., Wang, X. X., Lin, S. Q., Zhang, L. H., Lin, C. Q., Li, Z. M., Liu, J. M. (2012). Research on the spectral properties of luminescent carbon dots. Spectrochimica Acta Part A: Molecular and Biomolecular Spectroscopy, 95, 555–561.

Liu, J., Liu, Y., Liu, N., Han, Y. Z., Zhang, X., Huang, H., … Kang, Z. H. (2015). Metal-free efficient photocatalyst for stable visible water splitting via a two-electron pathway. Science, 347, 970–974.

Molaei, M. J. (2019). Carbon quantum dots and their biomedical and therapeutic applications: a review. RSC Advances, 9, 6460-6481.

Murru, C., Badía-Laíño, R., Díaz-García, M.E. (2020). Synthesis and characterization of green carbon dots for scavenging radical oxygen species in aqueous and oil samples. Antioxidants, 9, 1147-1164.

Nandiyanto, A.B. D., Oktiani, R., Ragadhita, R. (2019). How to read and interpret FTIR spectroscope of organic material. Indonesian Journal of Science & Technology, 4, 97-118.

Nikolic, G. S., Zlatkovic, S. Z. (2010). Assaying the variation in secondary metabolites of St. John's Wort for its better use as an antibiotic. Journal of Medicinal Plants Research, 4, 211.

Önal, Y., Kır, Ş., Dehri, İ., Esen, R. (2019). Synthesis and characterization of graphene quantum dots from dried pine leaves. Journal of Turkish Chemical Society Chemical Engineering B, 2, 109-120.

Pandiyan, S., Arumugam, L., Srirengan, S. P., Pitchan, R., Sevugan, P., Kannan, K., …Gandhirajan, V. (2020). Biocompatible carbon quantum dots derived from sugarcane industrial wastes for effective nonlinear optical behavior and antimicrobial activity applications. ACS Omega, 5(47), 30363-30372.

Peer, D., Karp, J. M., Hong, S., Farokhzad, Q. C., Margalit, R., Langer, R. (2007). Nanocarriers as an emerging platform for cancer therapy. NatureNanotechnology, 2, 751–760.

Pohanka, M. (2017). Quantum dots in the therapy:current trends and perspectives. Mini Reviews in Medicinal Chemistry, 17, 650-656.

Shahla, A. F. F., Masoud, S. N., Davood, G. (2018). Hydrothermal green synthesis of magnetic Fe_3O_4-carbon dots by lemon and grape fruit extracts and as a photoluminescence sensor for detecting of E. coli bacteria. Spectrochimica Acta Part A: Molecular and Biomolecular Spectroscopy, 203, 481–493.

Taraj, K., Cıko, L., Malollari, I., Andoni, A., Ylli, F., Ylli, A., … Borshi, XH. (2019). Eco-extraction of essential oil from albanian hypericum perforatum l. and characterisation by spectroscopy techniques. Journal of Environmental Protection and Ecology, 20, 188-195.

Tian, L., Ghosh, D., Chen, W., Pradhan, S., Chang, X. J., Chen, S. W. (2009). Nanosized carbon particles from natural gas soot. Chemistry of Materials, 21, 2803–2809.

Wagner, A. M., Knipe, J. M., Orive, G., Peppas, N. A. (2019). Quantum dots in biomedical applications. Acta Biomateralia, 94, 44-63.

Wang. L., Zhou, H. S. (2014). Green synthesis of luminescent nitrogen-doped carbon dots from milk and its imaging application. Analtical Chemistry, 86, 8902–8905.

Wang, Q., Liu, X., Zhang, L. C., Lv, Y. (2012). Microwave-assisted synthesis of carbon nanodots through an eggshell membrane and their fluorescent application. Analyst, 137, 5392–5397.

Xu, X. Y., Ray, R., Gu, Y. L., Ploehn, H. J., Gearheart, L., Raker, K., Scrivens, W. A. (2004). Electrophoretic analysis and purification of fluorescent single-walled carbon nanotube fragments. Jornal of American Chemical Society, 126, 12736–12737.

Xue, B., Yang, Y., Sun, Y., Fan, J., Li, X., Zhang, Z. (2019). Photoluminescent lignin hybridized car- bon quantum dots composites for bioimaging applications. International Journal of Biological Macromolecus, 122, 954–961.

Yang, S. T., Cao, L., Gao, P. J., Lu, F. S., Wang, X., Wang, H. F., …Sun, Y. P. (2009). Carbon dots for optical imaging in vivo. Journal of the American Chemical Society, 131(32), 11308–11309.

Yong, K. T. (2009). Mn-doped near-infrared quantum dots as multimodal targeted probes for pancreatic cancer imaging. Nanotechnology, 20(1), 015102.

Zarrinbakhsh, N., Mohanty, A. K., Misra, M. (2013). Fundamental studies on water-washing of the corn ethanol coproduct (DDGS) and its characterization for biocomposite applications. Biomass Bioenergy, 55, 251–259.

Zheng, X. T., Ananthanarayanan, A., Luo, K. Q., Chen, P. (2015). Glowing graphene quantum dots and carbon dots: properties, syntheses, and biological applications. Small, 11, 1620-1636.